This is an open access article published under an ACS AuthorChoice License, which permits copying and redistribution of the article or any adaptations for non-commercial purposes.

Inorganic Chemistry

Article

pubs.acs.org/IC

A New Look at the Structural Properties of Trisodium Uranate Na_3UO_4

Anna L. Smith,*[†,‡] Philippe E. Raison,*[†] Laura Martel,[†] Damien Prieur,[†] Thibault Charpentier,[§] Gilles Wallez,[∥,⊥] Emmanuelle Suard,[#] Andreas C. Scheinost,[○] Christoph Hennig,[○] Philippe Martin,[▽] Kristina O. Kvashnina,[◆] Anthony K. Cheetham,[‡] and Rudy J. M. Konings[†]

[†]European Commission, Joint Research Centre, Institute for Transuranium Elements, P.O. Box 2340, D-76125 Karlsruhe, Germany

[‡]Department of Materials Science and Metallurgy, University of Cambridge, 27 Charles Babbage Road, Cambridge, CB3 0FS, United Kingdom

[§]UMR CEA/CNRS 3685 − NIMBE, 91191 Gif-sur-Yvette, France

[∥]PSL Research University, Chimie ParisTech−CNRS, Institut de Recherche de Chimie Paris, 75005 Paris, France

[⊥]Sorbonne University, UPMC Université Paris 06, 75005 Paris, France

[#]Institut Laue Langevin, Rue Jules Horowitz, BP 156, 38042, Grenoble cedex 9, France

[○]Helmholtz Zentrum Dresden Rossendorf (HZDR), Institute of Resource Ecology, P.O. Box 10119, 01314 Dresden, Germany

[▽]CEA, DEN, DEC, CEN Cadarache, 13108 St. Paul Lez Durance, France

[◆]European Synchrotron Radiation Facility, 6 rue Jules Horowitz, BP 220, 38043 Grenoble, France

Supporting Information

ABSTRACT: The crystal structure of trisodium uranate, which forms following the interaction between sodium and hyperstoichiometric urania, has been solved for the first time using powder X-ray and neutron diffraction, X-ray absorption near-edge structure spectroscopy, and solid-state ^{23}Na multiquantum magic angle spinning nuclear magnetic resonance. The compound, isostructural with Na_3BiO_4, has monoclinic symmetry, in space group $P2/c$. Moreover, it has been shown that this structure can accommodate some cationic disorder, with up to 16(2)% sodium on the uranium site, corresponding to the composition α-$Na_3(U_{1-x},Na_x)O_4$ ($0 < x < 0.18$). The α phase adopts a mixed valence state with the presence of U(V) and U(VI). The two polymorphs of this compound described in the literature, m- and β-$Na_3(U_{1-x},Na_x)O_4$, have also been investigated, and their relationship to the α phase has been established. The completely disordered low-temperature cubic phase corresponds to a metastable phase. The semiordered high-temperature β phase is cubic, in space group $Fd\bar{3}m$.

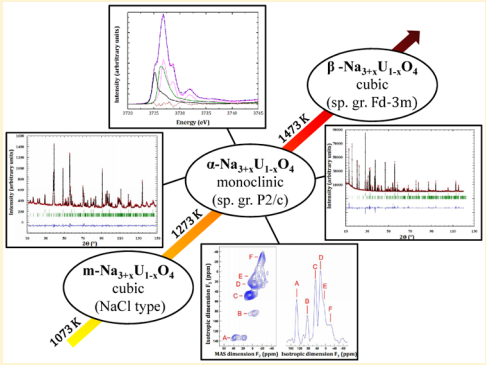

INTRODUCTION

Sodium-cooled fast reactors (SFRs) are considered to be a promising option for the next generation of nuclear reactors by the Generation IV International Forum (GIF).[1] One significant safety concern regarding these reactors comes from the potential interaction of the sodium metallic coolant with the $(U,Pu)O_2$ fuel in the event of a breach of the stainless steel cladding.[2−4] Past experimental work carried out in the 1980s on the reaction between liquid sodium, urania, and urania−plutonia solid solutions has shown that in the temperature range of the fuel during operation, close to the pellet rim (around 923 K), the main reaction products were of formula Na_3MO_4, where M = $(U_{1-x}Pu_x)$.[5−9] The compound Na_3MO_4 was found to be of much lower density (5.6 g·cm^{-3}) and to have less than half the thermal conductivity relative to the mixed oxide,[2−4,10] leading to local swelling and temperature increase in the fuel pin, with the potential threat of further cladding failure.[2−4]

The technological importance of the sodium urano-plutonate has led to a considerable interest in its structural[11−15] and thermodynamic[16−18] properties. With the plutonium concentration in the $(U,Pu)O_2$ fuel being typically on the order of 20 wt %, the compounds Na_3UO_4 and $Na_3(U_{1-x},Pu_x)O_4$ are expected to be isostructural and have similar thermomechanical and thermodynamic properties.[5−9] However, the crystal structure of Na_3UO_4 has remained the subject of controversy up to now.[14]

Scholder and Gläser[11] first reported in 1964 a disordered NaCl type of structure, obtained at low temperatures ($T < 973$

Received: January 20, 2015
Published: March 23, 2015

 © 2015 American Chemical Society

DOI: 10.1021/acs.inorgchem.5b00136
Inorg. Chem. 2015, 54, 3552−3561

K), with a cell parameter of 4.77 Å (*m* phase). In 1970, Bartram and Fryxell[12] obtained, at temperatures ranging from 973 to 1273 K, a new phase named α, ordered this time with many additional reflections, and they assigned it to cubic symmetry with a doubled cell parameter, 9.54 Å, and the chemical composition $Na_{11}U_5O_{16}$. The latter composition was ruled out by Lorenzelli et al.[14] in 1985, however, as their own X-ray diffraction pattern showed many additional reflections that were not taken into account by Bartram and Fryxell, and that could not belong to a cubic structure. According to them, the correct composition is Na_3UO_4, although their attempts to index it in tetragonal and orthorhombic systems were not successful. In 1972, Marcon et al.[13] discovered the formation of a high-temperature (>1273 K), partially ordered cubic phase of Na_3UO_4, named β, with space group $Fd\bar{3}m$ and a cell parameter of 9.56 Å. Lorenzelli et al. confirmed those results and established a reversible phase transition between the α and β forms around (1348 ± 25) K. Finally, Pillon revisited the question in 1989[15] and 1993[19] by means of X-ray diffraction coupled to neutron diffraction and microcalorimetry for quantitative analysis of the sodium formed during the reaction. On the basis of the latter quantitative analysis, the formation of a metastable intermediate tetravalent uranate Na_4UO_4 was described for temperatures below 848 K by direct reaction between UO_2 and Na_2O, followed by a decomposition reaction above 873 K with progressive loss of sodium toward the $Na_{3+x}UO_4$ composition. The structure of this metastable intermediate Na_4UO_4 phase was described as fcc, very close to the structure of Scholder and Gläser,[11] with a cell parameter of 4.78 Å, and the decomposition reaction to Na_3UO_4 was shown to be irreversible. To the authors' knowledge, no other studies have been reported since the work of Pillon et al.,[19] and the discrepancies have remained.

In the present work, we have solved the structure of the α phase of the trisodium uranate using powder X-ray diffraction coupled to neutron diffraction, X-ray absorption near-edge structure (XANES), and ^{23}Na magic angle spinning (MAS) nuclear magnetic resonance (NMR). We have also established that excess sodium can be incorporated in this structure, up to the composition $Na_{3.16(2)}U_{0.84(2)}O_4$, which was never considered in past studies. The phase relationships between α and its two polymorphs *m* and β have finally been investigated.

■ EXPERIMENTAL SECTION

Raw Materials and Solid-State Synthesis. Depleted uranium dioxide (UO_2 from JRC-ITU stocks) was ground together with sodium oxide (Na_2O 82.1% + Na_2O_2 14.8%, ABCR GmbH & Co, i.e., $Na_2O_{1.14(1)}$) in a $UO_2/Na_2O_{1.14(1)}$ = 1:2.1 ratio in an argon-filled dry glovebox. Sodium oxide was carefully stored in the dry atmosphere of the glovebox because of its hygroscopic nature. The starting uranium dioxide, being hyperstoichiometric,[20] was first reduced to stoichiometry under Ar/6% H_2 flow at 993 K for 8 h. The X-ray pattern revealed a single cubic phase with fluorite structure and a cell parameter of 5.469(3) Å. This is in good agreement with the value reported in the literature,[20] indicating that the starting uranium dioxide was very close to stoichiometry after thermal treatment.

The ($UO_2/Na_2O_{1.14(1)}$) mixture was then introduced into stainless steel containers that were tightly closed under the purified argon atmosphere of the glovebox and heated in a tubular furnace at 1073 (12 h), 1173 (24 h), and 1273 K (24 h) for the *m*, β, and α phases, respectively. The α phase, synthesized at 1273 K, was also heated at 1483 K for 30 min, 1 h, and 3 h, successively, and analyzed by X-ray diffraction after each thermal treatment.

The α compound was obtained together with about 21.8 wt % unreacted uranium dioxide according to X-ray diffraction characterization. Under the specified temperature and oxygen potential conditions, it was not possible to suppress the uranium dioxide secondary phase. Indeed, the reaction performed in a $UO_2/Na_2O_{1.14(1)}$ = 1:1.8 ratio led to the same product and to unreacted uranium dioxide, according to the cell parameters determination.

X-ray Diffraction. The crystal structures of the synthesized compounds were determined at room temperature by X-ray diffraction (XRD) using a Bruker D8 Advance X-ray diffractometer mounted in the Bragg−Brentano configuration with a curved Ge monochromator (111) and a copper tube (40 kV, 40 mA) equipped with a LinxEye position sensitive detector. The data were collected by step scanning in the angle range $10° \leq 2\theta \leq 120°$, with an integration time of about 8 h, a count step of 0.02° (2θ), and a dwell of 5 s/step. The sample preparation for XRD analysis involved dispersing the powder on the surface of a silicon wafer with 2 or 3 drops of isopropanol. Structural analysis was performed by the Rietveld method with the Fullprof2k suite.[21]

Neutron Diffraction. Neutron diffraction patterns were recorded at the Institut Laue Langevin (ILL, Grenoble) on the instrument D2B with 1.1 g of α-phase sample prepared at the ITU. The sample was encapsulated in an hermetic vanadium container tightly closed with an indium joint. The data were collected at a fixed wavelength (λ = 1.594 Å) over 48 h by step scanning in the angle range $0° \leq 2\theta \leq 160°$. Each step corresponded to 0.05° in 2θ as the 128 detectors are spaced at 1.25° intervals.

X-ray Absorption Near-Edge Structure (XANES) Spectroscopy. XANES measurements were performed both at the Rossendorf BeamLine (ROBL, Beamline 20) and beamline ID26[22] of the European Synchrotron Radiation Facility (ESRF) in Grenoble (France). In both cases, small amounts (5−10 mg) of powdered sample were mixed with boron nitride (BN) and pressed into pellets for XANES measurements. The storage ring operating conditions were 6.0 GeV and 170−200 mA.

Experimental Conditions at ROBL. A double crystal monochromator mounted with a Si(111) crystal coupled to collimating and focusing Rh coated mirrors was used. XANES spectra were collected at room temperature in the transmission mode at the U-L_3 edge. A step size of 0.5 eV was used in the edge region. The E_0 values were taken at the first inflection point by using the first node of the second derivative. The position of the white-line maximum was selected from the first node of the first derivative. Several acquisitions were performed on the same sample and summed to improve the signal-to-noise ratio. Before averaging the scans, each spectrum was aligned using the XANES spectra of a metallic yttrium foil (17038 eV). The ATHENA software[23] was used to remove the background and to normalize the spectra.

Experimental Conditions at ID26. The incident energy was selected using the (111) reflection from a double Si crystal monochromator. Rejection of higher harmonics was achieved by three Si mirrors at an angle of 3.5 mrad relative to the incident beam. XANES spectra were measured in high-energy-resolution fluorescence detected (HERFD) mode using an X-ray emission spectrometer.[24] The sample, analyzer crystal, and photon detector (silicon drift diode) were arranged in a vertical Rowland geometry. The U HERFD spectra at the M_4 edge were obtained by recording the maximum intensity of the U $M\beta$ emission line (∼3337 eV) as a function of the incident energy. The emission energy was selected using the (220) reflection of the five spherically bent Si crystal analyzers (with 1 m bending radius) aligned at 75° Bragg angle. The paths of the incident and emitted X-rays through air were minimized in order to avoid losses in intensity due to absorption. The intensity was normalized to the incident flux. A combined (incident convoluted with emitted) energy resolution of 0.7 eV was obtained, as determined by measuring the full width at half-maximum (fwhm) of the elastic peak. The present data is not corrected for self-absorption effects. The analysis shown in this work is based on comparison of the energy position of the main transitions at the U-M_4 edge, which is affected only very slightly by self-absorption effects.

^{23}Na Magic Angle Spinning (MAS) Nuclear Magnetic Resonance (NMR). The ^{23}Na MAS NMR spectra were measured at

DOI: 10.1021/acs.inorgchem.5b00136
Inorg. Chem. 2015, 54, 3552−3561

a Larmor frequency of 105.8 MHz on the 9.4 T Bruker spectrometer installed at the JRC-ITU.[25] A 1.3 mm probe was used, and the rotor spun at 55 kHz. A radiofrequency-field of 42 kHz ($\pi/2$, 48 transients with a 0.5 s relaxation delay) was applied to be in the selective excitation regime. To improve the spectral resolution of the ^{23}Na quadrupolar nucleus ($S = {}^3/_2$), rotation-induced adiabatic coherence transfer (RIACT) multiquantum magic angle spinning (MQMAS) experiments[26] were acquired with optimization excitation and reconversion pulses p_1 = 2.5 μs and p_2 = 4.5 μs. The obtained two-dimensional MQMAS spectra yield the MAS spectrum in the direct dimension (F_2) and the isotropic spectrum, which is free of second-order quadrupolar anisotropic broadening, in the indirect dimension (F_1). All ^{23}Na shifts were referenced to 1 M NaCl (aq). Spectra were processed using an in-house developed code.[27]

Differential Scanning Calorimetry. Differential scanning calorimetry measurements were performed with a SETARAM MDHTC96 apparatus equipped with a furnace and a detector monitoring the difference in heat flow between sample and reference crucibles. The α-phase material (110.9 mg) was encapsulated for the measurement in stainless steel crucibles with a screwed bolt to avoid vaporization as described in another publication.[28] The crucibles were brought to 1483 K with a heating rate (respectively cooling rate) of 10 K/min. The temperature was monitored throughout the experiment by a series of interconnected S-types thermocouples.

■ RESULTS AND DISCUSSION

Study of the Low-Temperature *m*-Phase Compound. The cubic structure as described by Scholder and Gläser[11] (a = 4.77 Å for Na_3UO_4) and Pillon[19] (a = 4.78 Å for Na_4UO_4) was obtained in the present study at relatively low temperatures (1073 K) after a short thermal treatment (12 h) (X-ray diffraction pattern is shown in the Supporting Information). The unit cell parameter of this NaCl type of structure was determined at a = 4.764(3) Å with a Le Bail fit (Table 6), in good agreement with the reported values. The structure appears to be completely disordered, with Na and U randomly distributed throughout the cationic sites. As reported in the work of Lorenzelli et al.,[14] one would expect this compound with complete disorder to correspond to a high-temperature γ form. The authors could not observe it up to 1400 K, however, and systematically obtained the α form described in the next section in the temperature ranges of Scholder and Gläser. It is hence suggested that this cubic compound, with cell parameter a = 4.764(3) Å, corresponds to a metastable rather than to an equilibrium phase, which forms when insufficient time is given for ordering.

A XANES spectrum of this compound was collected at the ID26 beamline at the U-M_4 edge to determine its uranium valence state. Figure 1 shows the recorded data together with UO_2, U_4O_9, U_3O_8, and UO_3 reference materials measured at the same beamline.[29] UO_2 and UO_3 correspond to pure U(IV) and U(VI), respectively, whereas U_4O_9 and U_3O_8 are mixed-valence U oxides with (${}^1/_2$ U(IV) + ${}^1/_2$ U(V)) for the former and (${}^2/_3$ U(V) + ${}^1/_3$ U(VI)) for the latter.[29] Kvashnina et al. performed a detailed description of the specific features for each compound, in particular with respect to the spectral shape and energy positions of the white lines (corresponding to the resonance of the absorption spectra).[29] The main resonances for these compounds are listed in Table 1.

The measured m phase clearly ressembles that of UO_3, with three main resonances at ~3726.9, ~3728.6, and ~3731.9 eV. The second feature is usually attributed to the characteristic feature of the uranyl ion.[29] Surprisingly, the synthesized m phase can be attributed to the pure U(VI) valence state, although a U(V) state was originally expected. However, the

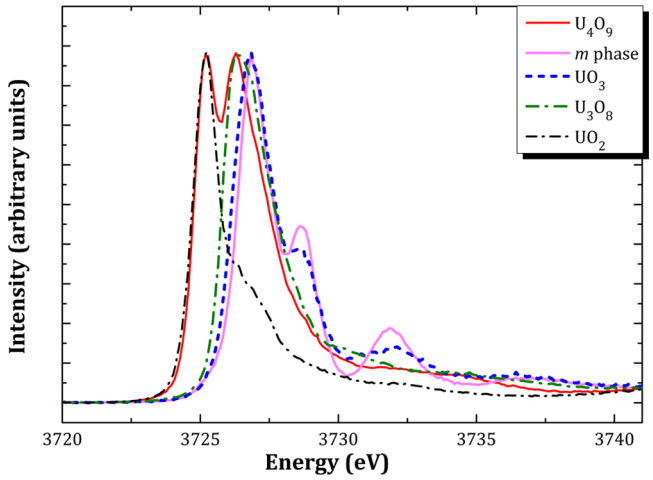

Figure 1. XANES spectrum of the m phase measured at the U-M_4 edge and comparison with the reference spectra of UO_2, U_4O_9, U_3O_8, and UO_3.[29]

absence of any feature at ~3726.3 eV completely rules out the possibility of such an assignment.[29] These results lead to the conclusion that the prepared product does not correspond to the $Na_3U^VO_4$ composition but rather $Na_4U^{VI}O_5$. The existence of the m-Na_4UO_5 cubic phase was reported in the literature with a cell parameter of 4.766 Å,[30] but is a subject of controversy.[31,32] The present work confirms its existence and agrees on the determination of its cell parameter (a = 4.764(3) Å herein). The existence of the m-Na_3UO_4 phase cannot be substantiated from our findings, however. We can suggest applying more reducing conditions during the synthesis to reach this composition, such as using a zirconium liner acting as an oxygen pump or adding sodium metal above the (UO_2/Na_2O) mixture. Complementary studies are needed to clarify this point.

Recent data acquired on sodium uranate compounds have shown that ^{23}Na MAS NMR measurements could also indirectly yield some information on the uranium valence state. A paramagnetic shift of the ^{23}Na signal was indeed observed for NaU^VO_3, whereas β-$Na_4U^{VI}O_5$ and $Na_2U^{VI}{}_2O_7$ followed diamagnetic behavior.[33] The ^{23}Na MAS NMR spectrum of the synthesized m phase is presented in Figure 2. It shows a very sharp contribution, which can be attributed to a very symmetric sodium environment, probably coming from the partial decomposition of the compound. The isotropic chemical shift is within the diamagnetic range of ^{23} Na, which further argues for a purely U(VI) phase. The ^{23}Na MQMAS spectrum is shown in Figure 3, which presents an important broadening. This feature can be related to the complete disorder of the m phase, meaning that all of the sodium sites are shared with uranium.

Study of the α-Phase Compound. *Powder X-ray Diffraction.* The phase described by Bartram and Fryxell[12] (α phase), to which a cubic structure (a = 9.54 Å) was first attributed, was synthesized at 1273 K. X-ray diffraction and structural refinement showed that about 21.8 wt % of uranium dioxide remained as unreacted product with a cell parameter of 5.471(3) Å, in very good agreement with the literature for stoichiometric uranium dioxide.[20] A number of Bragg reflections at 2θ values of 30.66, 37.10, 39.50, 40.94, 48.10, 48.33, 48.95, 50.75, 50.88, 51.17, 51.31, and 54.65° were not reported by Bartram and Fryxell, whereas others appeared to be

DOI: 10.1021/acs.inorgchem.5b00136
Inorg. Chem. 2015, 54, 3552−3561

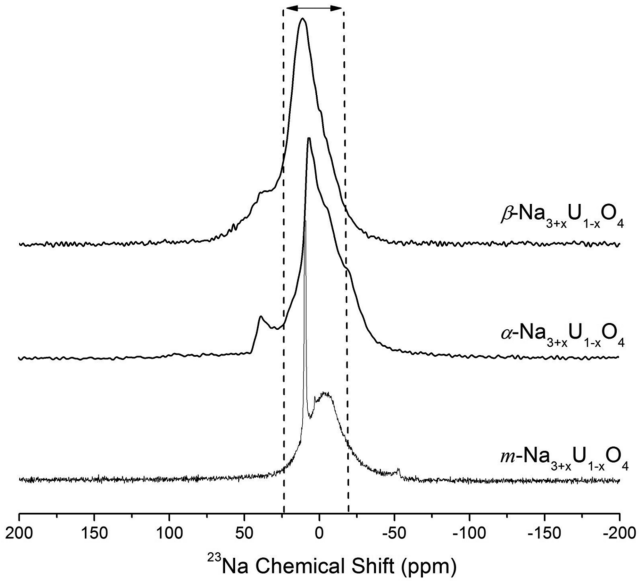

Figure 2. ^{23}Na MAS NMR spectra of the synthesized *m*, *α*, and *β* phases ($0 < x < 0.2$). The region between the dashed lines represents the range of isotropic chemical shift values in which ^{23}Na does not present a paramagnetic shift.[33]

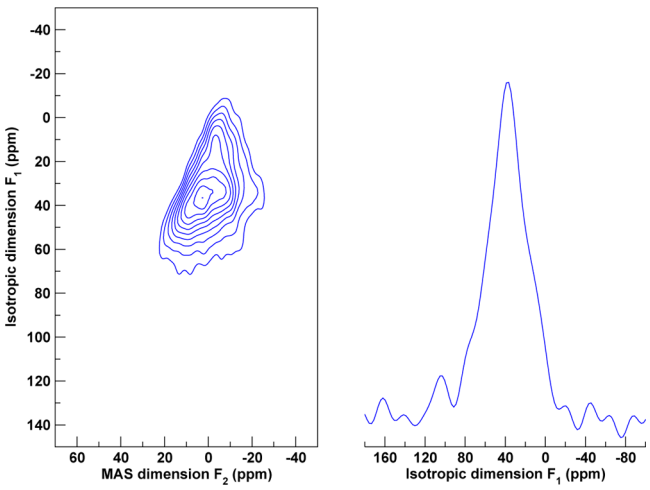

Figure 3. ^{23}Na MQMAS spectra of the synthesized *m*-Na_4UO_5 phase and projection along the isotropic dimension F_1.

shifted (the 211 reflection, for example, reported at 22.81° and observed at 22.61°), and some did not appear at all (the 200 reflection reported at 18.59°). In accordance with the assumptions of Lorenzelli et al.,[14] we concluded that the structure could not be simple cubic. An ab initio structure determination using the program *NTREOR* implemented in *EXPO2013*[34] in conjunction with the FIZ/NIST Inorganic Crystal Structure Database (ICSD) revealed a monoclinic unit cell. It was found that the *α* compound is isostructural with Na_3BiO_4,[35] which has space group *P*2/*c* (N° 13). The Na_3BiO4 structure, which is completely ordered, corresponds to one bismuth site in Wyckoff position (2e), three sodium sites in positions (2e), (2f), and (2f), respectively, and two oxygen sites in Wyckoff position (4*g*).

XANES Spectroscopy. A XANES spectrum of the aforementioned *α* phase was collected at the U-L_3 edge together with that of $U^{IV}O_2$,[36] $NaU^{V}O_3$,[37] and $Na_4U^{VI}O_5$[33] reference compounds to determine the valence state of uranium. The recorded spectra and the energy positions of the inflection points and of the white lines are provided in the Supporting Information.

The inflection point and white lines of the *α*-phase material were found to be between those of UO_2 and Na_4UO_5. Furthermore, the experimental spectrum revealed a shoulder about 15 eV after the white line and reduced peak amplitude, which is a characteristic feature of an uranyl type of configuration observed in U(VI).[36] The U(IV), U(V), and U(VI) molar fractions were subsequently determined by fitting the experimental data using a linear combination of $U^{IV}O_2$, $NaU^{V}O_3$, and $Na_4U^{VI}O_5$ XANES reference spectra.[33] The linear combination fit, which is shown in the Supporting Information, yielded 24(3)% and 76(3)% U(IV) and U(VI), respectively, but no U(V). The U(IV) molar fraction found herein, corresponding to the UO_2 secondary phase, is in good agreement with the amount determined by X-ray diffraction (about 21.8 wt % in weight fractions, i.e., 25.9% in molar fractions). This XANES study hence suggested that the synthesized *α* phase presented a significant fraction of U(VI) and was not made exclusively of U(V), as expected for the Na_3UO_4 stoichiometric composition.

The chemical shift between the inflection points of $U^{IV}O_2$ (17169.9(5) eV) and $NaU^{V}O_3$ (17170.4(5) eV) reference materials measured at the U-L_3 edge was found to be ∼0.5 eV only. As a consequence of the short core hole lifetime at the U $2p_{3/2}$ level, the natural width of the L_3 level, causing spectral line broadening, amounts to 7.43 eV. This means that small U(V) concentrations present in the *α* phase could not be detected at this edge given that it is mixed with about 25.9% uranium dioxide in the investigated material. The measurement was therefore repeated at the U-M_4 edge (at beamline ID26), where the core hole lifetime braodening is less pronounced than that at the U-L_3 edge.

The XANES spectrum recorded at the U-M_4 edge is shown in Figure 4a together with the spectra of reference materials. The energy positions of the main resonances for those compounds are listed in Table 1. The experimental data for the *α*-phase material shows four peak maxima at ∼3725.3, ∼3726.8, ∼3728.7, and ∼3731.9 eV. The first one is clearly due to the uranium dioxide secondary phase, whereas the three other ones are features related to U(VI). A linear combination fitting was again carried out using the reference materials. The spectrum obtained for the *m*-Na_4UO_5 phase shown in the previous section was used as a reference for U(VI) instead of UO_3. This gave a better quality fit as could be expected from the greater similarities in local structure around the uranium cation in the *α* and *m* phases compared to UO_3. The best result, which is shown in Figure 4b, was obtained for 27.7% UO_2, 33.2% U_3O_8, and 39.1% *m*-Na_4UO_5. The UO_2 fraction is in very good agreement with the one determined by X-ray diffraction (25.9%). According to this analysis, the synthesized material hence corresponds to (27.7 ± 6%) U(IV), (22.3 ± 6%) U(V), and (50.1 ± 6%) U(VI), whereas the *α* phase itself is made of (31 ± 6%) U(V) and (69 ± 6%) U(VI). An attempt was made to perform a linear combination with U(IV) and U(VI) only, but the calculated residual difference between experimental data and fit then showed a maximum around the energy of U(V). The mean valence state deduced from those measurements for the *α* phase is finally +5.69(6).

Structural Refinement Using Neutron Diffraction and Evidence for Structural Disorder. XANES analysis of the synthesized *α* phase at the U-L_3 and U-M_4 edges has shown

DOI: 10.1021/acs.inorgchem.5b00136
Inorg. Chem. 2015, 54, 3552−3561

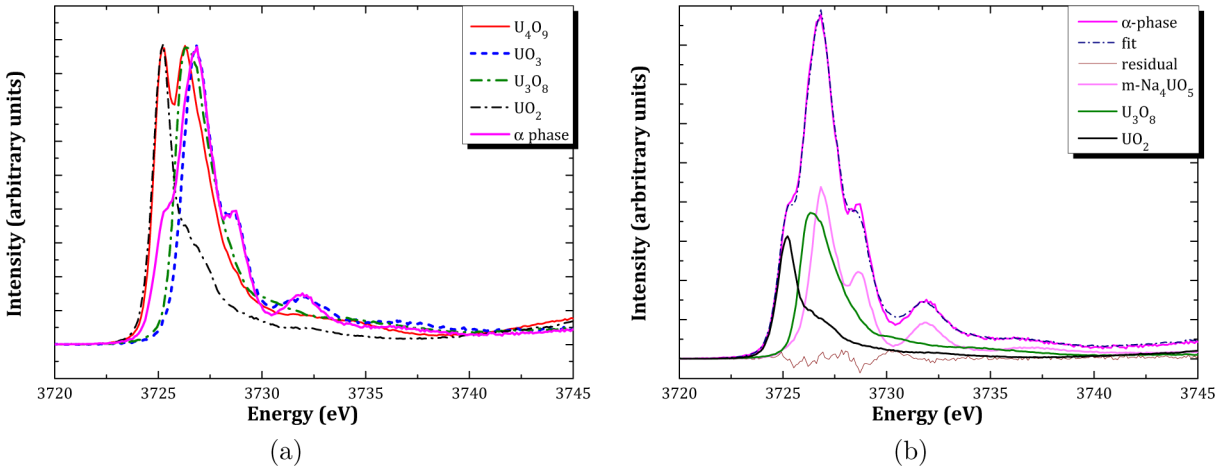

Figure 4. (a) XANES spectrum of the synthesized α-phase material measured at the U-M_4 edge and comparison with the reference spectra of UO_2, U_4O_9, U_3O_8, and UO_3.[29] (b) XANES spectrum of the synthesized α-phase material and its fit together with the weighted components used in the linear combination.

Table 1. Energie Positions of the Main Resonances of the U-M_4 XANES Spectra

sample	resonance positions (eV)				
UO_2	3725.2(3)				
U_4O_9	3725.2(3)	3726.3(3)			
U_3O_8		3726.4(3)			
UO_3			3726.8(3)	3728.6(3)	3732.1(3)
m-Na_4UO_5			3726.9(3)	3728.6(3)	3731.9(3)
α phase	3725.3(3)		3726.8(3)	3728.7(3)	3731.9(3)

that the structural model should account for the existence of U(VI). The Na_3BiO_4 starting model, corresponding to a perfectly ordered structure and to a bismuth (respectively uranium) cation in the oxidation state (V), was therefore slightly modified.

The compensation of the U(VI) charge by creation of oxygen interstitials into the structure, i.e., corresponding to the composition Na_3UO_{4+x} ($0 < x < 0.5$), was first excluded. Indeed, no residual electronic density could be found on normally vacant sites when performing the calculation with the program GFourier of the Fullprof2k suite[21] as detailed below. Instead, the incorporation of excess sodium on the uranium Wyckoff site (2e) was tested, and the occupancy factors were refined. The refinement yielded an occupancy of 14−18% sodium together with 84−86% uranium. The structural model reported herein for the α phase hence corresponds to the $Na_3(U_{1-x},Na_x)O_4$ composition, written $Na_{3+x}U_{1-x}O_4$ with ($0.14 < x < 0.18$), where sodium shares the uranium site at a level of 14−18% occupancy. The corresponding X-ray and neutron diffraction refinements are shown in Figures 5 and 6.

The $Na_{3+x}U_{1-x}O_4$ formula with $x = 0$ and $x = 0.2$ corresponds to the Na_3UO_4 and Na_4UO_5 stoichiometric compositions, respectively. The synthesized α phase is hence found on the pseudobinary section between $Na_3U^VO_4$ and $Na_4U^{VI}O_5$ end-members, rather close to the latter composition, as shown in the phase diagram in Figure 7. The equilibrium β-Na_4UO_5 phase has a well-known tetragonal structure in space group $I4/m$,[38] so it is unlikely that α reaches the pure U(VI) valence state corresponding to the Na_4UO_5 composition. The $Na_{3.16(2)}U_{0.84(2)}O_4$ composition, found herein after refinement of the neutron data, corresponds to a mixed valence state compound with (76 ± 12%) U(VI) and (24 ± 12%) U(V). This is, moreover, in very good agreement with the

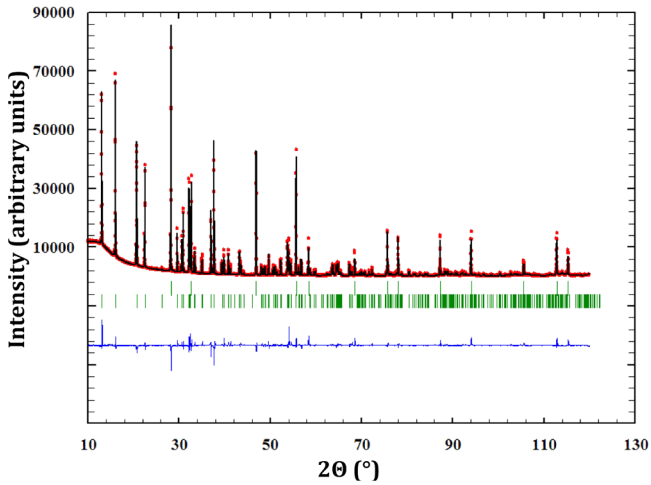

Figure 5. Comparison between the observed (Y_{obs}, in red) and calculated (Y_{calc}, in black) X-ray diffraction pattern of the α-$Na_3(U_{1-x},Na_x)O_4$ ($0.14 < x < 0.18$) phase. $Y_{obs} - Y_{calc}$, in blue, is the difference between the experimental and calculated intensities. The Bragg reflections are marked in green. Upper, UO_2; lower, α-$Na_3(U_{1-x},Na_x)O_4$. Measurement at $\lambda = 1.541$ Å.

stoichiometry derived from the linear combination fitting at the U-M_4 edge, i.e., $Na_{3.15(1)}U_{0.85(1)}O_4$ with (69 ± 6%) U(VI) and (31 ± 6%) U(V).

Rietveld refinement with the neutron data led to the following profile parameters: $a = 5.892(2)$ Å, $b = 6.772(2)$ Å, $c = 5.916(2)$ Å, and $\beta = 110.65(2)°$. Refined atomic positions are listed in Table 2. Selected bond lengths are listed in the Supporting Information.

DOI: 10.1021/acs.inorgchem.5b00136
Inorg. Chem. 2015, 54, 3552−3561

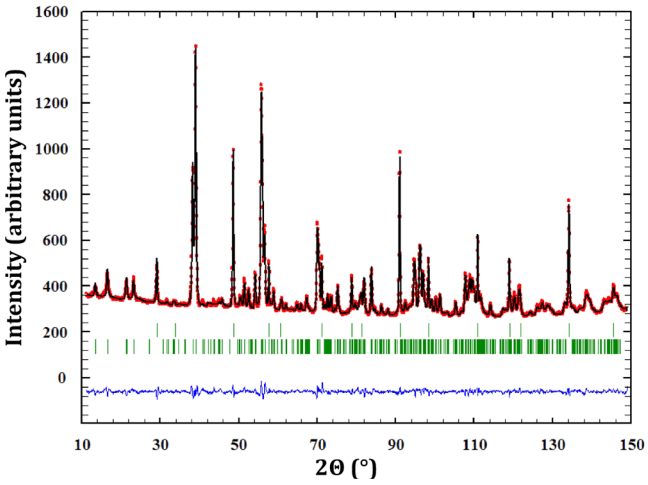

Figure 6. Comparison between the observed (Y_{obs}, in red) and calculated (Y_{calc}, in black) neutron diffraction pattern of the α-$Na_3(U_{1-x},Na_x)O_4$ ($0.14 < x < 0.18$) phase. $Y_{obs} - Y_{calc}$, in blue, is the difference between the experimental and calculated intensities. The Bragg reflections are marked in green. Upper, UO_2; lower, α-$Na_3(U_{1-x},Na_x)O_4$. Measurement at λ = 1.594 Å.

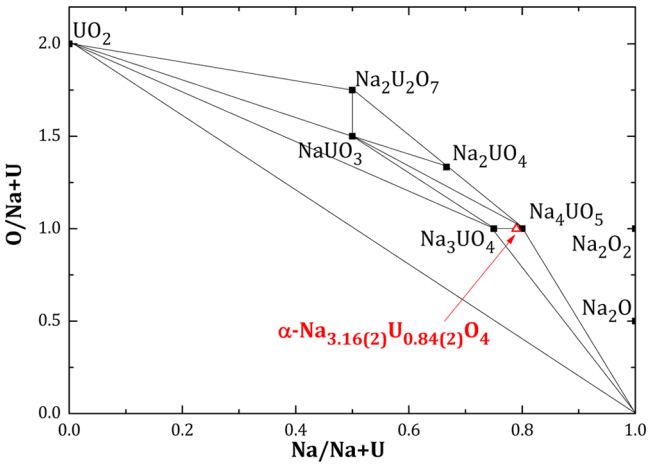

Figure 7. Ternary phase diagram Na−U−O. $Na_{3.16(2)}U_{0.84(2)}O_4$ is found on the pseudobinary section between Na_3UO_4 and Na_4UO_5.

The structure contains distorted UO_6 and NaO_6 octahedra. Looking at the *ac* plane, one can see that oxide layers alternate with sodium layers and layers shared between uranium and sodium atoms (Figure 8b). Moreover, the UO_6 octahedra share edges and form zigzag chains along *c* (Figure 8c), whereas the UO_6 and NaO_6 octahedra share edges with each other. The UO_6 octahedra are distorted with minimum and maximum bond lengths of 2.09(1) and 2.24(1) Å, respectively, whereas the variations are larger in the NaO_6 octahedra (from 2.34(1) to 2.78(1) Å). The bond angles in the UO_6 and NaO_6 octahedra vary from 166.64(1)° to 171.99(1)° and from 161.46(1)° to 175.05(1)°, respectively.

To test the validity of the former model, the residual electronic density remaining after refinement with the X-ray diffraction data was also calculated using the program GFourier of the Fullprof2k suite.[21] The refinement using the $Na_3U^VO_4$ model (corresponding to a perfectly ordered structure, isostructural with Na_3BiO_4) yielded a negative electronic density contribution on the uranium site (Figure 9a) at the level $z = 0.25$ (shown as a pink plane in Figure 8a), whereas the suggested refinement using the $Na_{3+x}U^{V,VI}{}_{1-x}O_4$ model ($0.14 < x < 0.18$) (presenting disorder on the uranium site) did not show any sign of a residue (Figure 9b). These results hence confirm the choice of the $Na_{3+x}U^{V,VI}{}_{1-x}O_4$ model ($0.14 < x < 0.18$) rather than Na_3UO_4 for the synthesized α phase and validate our structural model.

The results presented above have some significant implications from a safety perspective for the nuclear fuel−sodium interaction. Indeed, they suggest that the α phase of the fuel−sodium reaction product has some flexibility to incorporate excess sodium by substitution on the uranium site. The charge compensation is then realized by the uranium, which adopts a mixed valence state between U(V) and U(VI). Such a hypothesis was never considered in past studies. Pillon, who quantitatively measured the sodium formed by the reaction between UO_2 and Na_2O using microcalorimetry, supposed the tetravalent intermediate compound Na_4UO_4 was forming up to 848 K and evolved toward $Na_{3+x}UO_4$ at higher temperatures. Pillon's calorimetric measurements suggested a certain solubility of excess sodium in the Na_3UO_4 structure, but the author did not present independent evidence of the oxidation state of the uranium cation. It is possible that instead of having synthesized a mixed U(IV)/U(V) compound the author obtained a mixed valence U(V)/U(VI) phase. We believe that the synthesis of purely pentavalent trisodium uranate requires more reducing conditions than those used in the present work (using a zirconium liner or adding excess sodium metal to the mixture). Future studies should try to assess the extent of the $Na_3(Na_x,U_{1-x})O_4$ domain on the pseudobinary section between Na_3UO_4 and Na_4UO_5, as this is crucial information for the safety assessment of the nuclear fuel−sodium interaction.

^{23}Na MQMAS NMR Study and Confirmation of the Structural Disorder. To obtain more structural information, NMR experiments were conducted to probe the local environment of the sodium atoms. For stoichiometric trisodium uranate Na_3UO_4 presenting pentavalent uranium, with a

Table 2. Refined Atomic Positions in α-$Na_{3+x}U_{1-x}O_4$ ($0.14 < x < 0.18$) Synthesized at 1273 K from the Neutron Data[a]

atom	ox. state	Wyckoff	x	y	z	B_0 (Å^2)	occupancy
U0	+6	2e	0	0.1366(5)	0.25	0.29(1)	0.84(2)
Na0	+1	2e	0	0.1366(5)	0.25	0.29(1)	0.16(2)
Na1	+1	2e	0	0.6129(5)	0.25	0.92(1)	1
Na2	+1	2f	0.5	0.8854(5)	0.25	1.74(1)	1
Na3	+1	2f	0.5	0.4057(5)	0.25	1.48(1)	1
O1	−2	4g	0.2060(5)	0.0981(5)	−0.0015(5)	0.88(1)	1
O2	−2	4g	0.2339(5)	0.3479(5)	0.4683(5)	0.90(1)	1

[a] R_{wp} = 7.77; R_{exp} = 3.06; χ^2 = 6.44 (standard deviation = 3σ).

DOI: 10.1021/acs.inorgchem.5b00136
Inorg. Chem. 2015, 54, 3552−3561

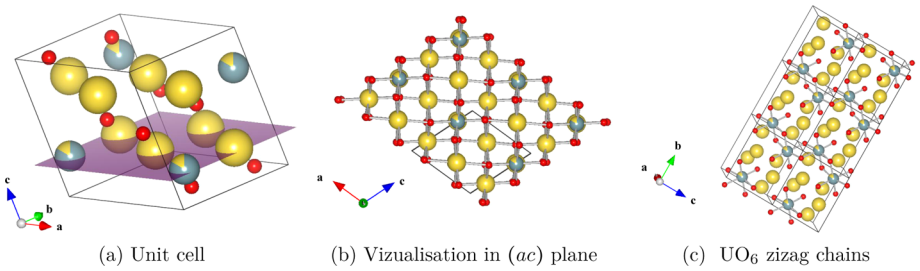

Figure 8. Drawing sketch of the α-$Na_{3+x}U_{1-x}O_4$ compound (U atoms are represented in gray, Na atoms, in yellow, and O atoms, in red): (a) unit cell, (b) vizualization in the *ac* plane, and (c) UO_6 zizag chains.

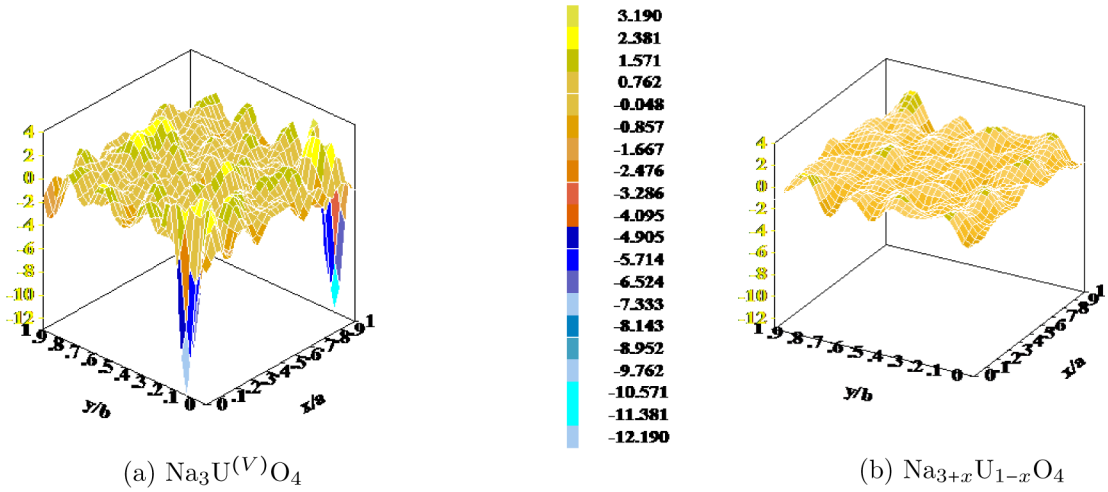

Figure 9. Residual electronic density ($F_{obs} - F_{calc}$) at $z = 0.25$ after refinement with the X-ray diffraction data for the two different models, i.e., (a) Na_3UO_4 and (b) $Na_{3+x}U_{1-x}O_4$ ($0.14 < x < 0.18$), using the program GFourier.

[Rn](5f^1) electronic structure, one would expect a paramagnetic shift of the sodium signal, as observed for NaU^VO_3.[33] For hexavalent uranium, corresponding to a [Rn](5f^0) electronic structure, diamagnetic behavior is expected as for $Na_4U^{VI}O_5$ and $Na_2U^{VI}{}_2O_7$.[33] The ^{23}Na MAS NMR spectrum of the synthesized α phase is presented in Figure 2. It is the sum of several ^{23}Na contributions, as the compound has three distinct sodium sites at Wyckoff positions, (2e), (2f), and (2f), plus one site (2e) shared with uranium as described previously.

As shown in Figure 2, the MAS spectrum shows a broad line with poor resolution. A ^{23}Na MQMAS experiment was therefore performed to improve the resolution. The ^{23}Na MQMAS spectrum, presented in Figure 10, shows three well-separated narrow sites (A, B, C), suggesting a well-ordered local environment, and a broad additional feature (D, E, F).

From the isotropic spectrum (Figure 10, right panel), the isotropic shift in the indirect dimension, δ_{ISO}, was extracted for each peak, and the center of gravity was calculated in the MAS dimension. The isotropic chemical shift, δ_{iso}, and quadrupolar product, P_Q, were subsequently derived as described in a previous work.[33] The corresponding parameters are summarized in Table 3. Because of the strong overlap between all of the lines and their ill-defined shapes (peaks D, E, and F), a fitting of the 1D MAS NMR spectrum was found to be too ambiguous to yield reliable quantification and was therefore not attempted in the present study.

Supposing that uranium is mostly in oxidation state (VI), as deduced from the XANES results and neutron refinement, peak A, at 47(5) ppm (Table 3), stands outside of the limits expected for a diamagnetic NaO_6 octahedron (23 ppm < δ_{iso} < −20 ppm).[33] Given the small contribution of this peak to the ^{23}Na MQMAS spectrum, it might be attributed to the U(V) fraction present in the α-phase compound. Furthermore, it is likely that peaks D, E, and F represent distorted NaO_6 octahedra types of sodium, whereas the remaining two more ordered signals (i.e., B and C) probably correspond to sodium sites shared with uranium. The ^{23}Na MQMAS spectrum therefore further confirms the existence of structural disorder in the synthesized α phase.

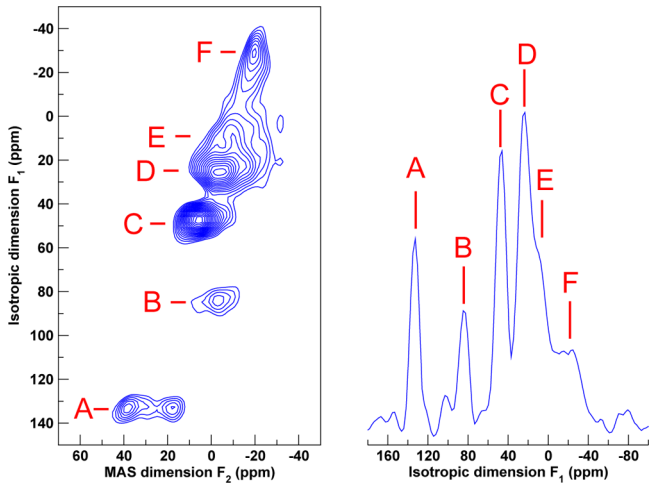

Figure 10. ^{23}Na MQMAS spectrum of the synthesized α phase and projection along the isotropic dimension F_1.

DOI: 10.1021/acs.inorgchem.5b00136
Inorg. Chem. 2015, 54, 3552−3561

Table 3. NMR Parameters Derived for the α Phase Using the Center of Gravity Method[33,a]

site	δ_{ISO} (ppm)	δ_{iso} (ppm)	P_Q (MHz)
A	133	47(5)	3.4(4)
B	84	18(5)	4.0(4)
C	46	13(5)	2.5(4)
D	24	2(5)	2.6(4)
E	9	−2(5)	2.2(4)
F	−17	−16(5)	2.4(4)

[a] δ_{ISO} is the isotropic shift in the indirect dimension of the MQMAS spectrum, δ_{iso} is the isotropic chemical shift, and P_Q is the quadrupolar parameter. Standard deviations are given in parentheses.

Study of the High-Temperature β Phase and Phase Relationship with the α Form. Differential scanning calorimetry (DSC) measurements were performed on the α phase in an attempt to visualize the phase transition to the high-temperature β phase as described by Marcon et al.[13] No thermal event could be detected when heating the sample up to 1483 K. However, the X-ray patterns recorded after 30 min, 1 h, and 3 h of thermal treatment at 1473 K revealed a progressive disappearance of the α phase and its replacement by β. The transition was complete after 3 h. From these results, it seems that the phase transition between the α and β forms is not instanteneous since it was not observed during the ramp of the DSC cycle, but rather slow and governed by kinetics. Lorenzelli et al.[14] observed the β phase after a long thermal treatment of the α phase (24 h at 1473 K and 70 h at 1393 K) followed by quenching, which also argues for such a hypothesis.

The β phase was also synthesized directly at a lower temperature (1173 K) in the present work together with about 1.70 wt % of unreacted uranium dioxide, which was rather unexpected. An explanation for this phenomenon could lie in the complex relationship between temperature and duration of synthesis and the degree of order/disorder in the structure. The X-ray diffraction pattern, shown in the Supporting Information, revealed a cubic structure (space group $Fd\overline{3}m$) with a cell parameter of 9.589(2) Å (Table 6), and not 9.56 Å as reported by Marcon et al.[13] The refined atomic positions found in the present work are given in Table 4. The proposed structural model corresponds to U(V), as our experimental data was unfortunately not sufficient to determine if excess sodium was present, which would correspond to a mixed valence state compound U(V)/U(VI).

The β structure is made of regular UO_6 and NaO_6 octahedra with U−O and Na−O bond lengths of 2.31(3) Å and 2.49(3) Å, respectively. A drawing of this structure is shown in the Supporting Information. This high-temperature form appears to be partially disordered, as uranium and sodium atoms share the (16c) site by 50%. The structural relationship between the α and β forms of the compound lies in the (U−Na3−U) diagonal of the monoclinic α unit cell, which corresponds to the (U,Na1−Na2−U,Na1) edge of the β unit cell. The sodium and uranium atoms along the diagonal are slightly misaligned but align themselves perfectly along the edge of the cubic cell when converting from one structure to the other.

The ^{23}Na MAS NMR spectrum of the synthesized β phase is presented in Figure 2. This is again the sum of several ^{23}Na contributions, as the structure possesses two distinct sodium sites. The ^{23}Na MQMAS spectrum is shown in Figure 11. The spectrum is consistent with two sites, even if it does not show them unequivocally. The MQMAS can resolve only one site (C′) with a broad line shape, typical of a disordered environment. The other contribution (B′) does not appear as clearly due to a lack of sensitivity (lower intensity and higher dispersion of NMR parameters), although it was clearly identified on the MAS spectrum. As was previously done for the α phase, the NMR parameters were extracted and are summarized in Table 5. The site (C′) stands within the limits of a diamagnetic NaO_6 octahedron (23 ppm < δ_{iso} < −20 ppm),[33] suggesting a mainly U(VI) valence state in the β phase compound. The site (B′) stands outside of these limits and could originate from the presence of U(V). These results

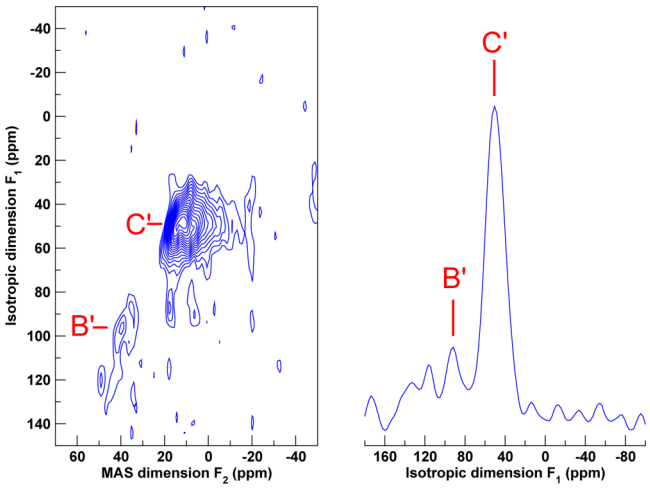

Figure 11. ^{23}Na MQMAS spectrum of the synthesized β-$Na_{3+x}U_{1-x}O_4$ phase and projection along the isotropic dimension F_1.

Table 5. NMR Parameters Derived for the β Phase Using the Center of Gravity Method[33,a]

site	δ_{ISO} (ppm)	δ_{iso} (ppm)	P_Q (MHz)
B′	92	31(10)	3.0(4)
C′	51	17(5)	2.3(4)

[a] δ_{ISO} is the isotropic shift in the indirect dimension of the MQMAS spectrum, δ_{iso} is the isotropic chemical shift, and P_Q is the quadrupolar parameter. Standard deviations are given in parentheses.

Table 4. Refined Atomic Positions in the β-$Na_{3+x}U_{1-x}O_4$ ($0 < x < 0.2$) Phase Synthesized at 1173 K[a]

atom	ox. state	Wyckoff	x	y	z	B_0 (Å^2)	occupancy
U	+5	16c	0	0	0	0.91(1)	0.5
Na1	+1	16c	0	0	0	0.91(1)	0.5
Na2	+1	16d	0.5	0.5	0.5	1.0	1
O	−2	32e	0.2406(8)	0.2406(8)	0.2406(8)	1.0	1

[a] R_{wp} = 18.0; R_{exp} = 6.38; χ^2 = 7.94 (standard deviation =3σ).

DOI: 10.1021/acs.inorgchem.5b00136
Inorg. Chem. 2015, 54, 3552−3561

therefore argue for a mixed valence state U(V)/U(VI) composition for the β compound, too. In addition, it is worth pointing out that the unit cell volume at room temperature of the synthesized β phase is almost exactly four times that of the synthesized α phase, suggesting no change in composition.

Finally, additional proof that the broadening observed in the α and β phases in the isotropic dimension arises from structural disorder, and more specifically from random Na/U substitution as evidenced by neutron diffraction, is obtained by comparison with the spectra of $NaU^{V}O_3$ and $Na_4U^{VI}O_5$ compounds.[33] In these cases, corresponding to well-crystallized and ordered samples with unequivocal valence states, the MQMAS spectra were characterized by a single narrow line in the isotropic dimension.

CONCLUSIONS

The present study has revisited the polymorphism of trisodium uranate Na_3UO_4. The cubic disordered structure of Scholder and Gläser[11] probably corresponds to a metastable *m* phase. The ordered α phase is monoclinic, in space group *P*2/*c*, whereas the semiordered high-temperature β phase is cubic, in space group $Fd\bar{3}m$ as described by Marcon et al.[13] The α structure was refined by the Rietveld method from X-ray and neutron diffraction data, thereby resolving the controversy in the literature.[14] We have shown that the α form can accommodate some cationic disorder up to 14−18% of sodium on the uranium site, i.e., corresponding to a mixed valence state compound with composition $Na_3(U_{1-x},Na_x)O_4$ ($0.14 < x < 0.18$) (Table 6).

Table 6. Profile Parameters for the Three Phases of $Na_{3+x}U_{1-x}O_4$ ($0 < x < 0.2$)

	α-$Na_{3.16(2)}U_{0.84(2)}O_4$	β-$Na_{3+x}U_{1-x}O_4$	*m*-Na_4UO_5
temp. (K)	298	298	298
λ (Å)	1.594	1.541	1.541
symmetry	monoclinic	cubic	cubic
Z	2	8	1
space group	*P*2/*c*	$Fd\bar{3}m$	$Fm\bar{3}m$
a (Å)	5.892(2)	9.589(2)	4.764(3)
b (Å)	6.772(2)	9.589(2)	4.764(3)
c (Å)	5.916(2)	9.589(2)	4.764(3)
α (deg)	90	90	90
β (deg)	110.65(2)	90	90
γ (deg)	90	90	90
cell volume (Å^3)	220.83(1)	881.91(1)	108.13(1)

This work illustrates the powerful combination of X-ray and neutron diffraction, XANES, and ^{23}Na MAS NMR in the solid state to solve complex structures at a very detailed level. If the X-ray diffraction technique provides a picture of the crystallographic structure, it does not give the signature of the oxidation state of the uranium and therefore the chemical composition of the compound. The degree of oxidation is a key parameter for the thermodynamic modeling of the system under accident conditions, as it relates to the oxygen potential in the fuel. Our combined analysis has revealed a certain solubility of excess sodium in the α phase, with partial substitution on the uranium site and concomitant charge compensation from U(V) to U(VI). The U(V)/U(VI) quantification obtained herein by neutron refinement corresponds to (76 ± 12%) U(VI) and (24 ± 12%) U(V), in very good agreement with the results obtained with the XANES measurement at the U-M_4 edge. The present experimental evidence that excess sodium can be incorporated into the fuel−sodium reaction product has evident consequences from a thermodynamic perspective and should be considered in future studies.

ASSOCIATED CONTENT

Supporting Information

X-ray crystallographic file in CIF format. Powder X-ray diffraction pattern of the *m* phase. XANES data of the α phase recorded at the U-L_3 edge. Selected bond lengths for the α-phase material after neutron refinement. Powder X-ray diffraction pattern of the β phase. This material is available free of charge via the Internet at http://pubs.acs.org.

AUTHOR INFORMATION

Corresponding Authors

*(A.L.S.) E-mail: anna.smith@ec.europa.eu.
*(P.E.R.) E-mail: philippe.raison@ec.europa.eu.

Notes

The authors declare no competing financial interest.

ACKNOWLEDGMENTS

The authors would like to express their gratitude to D. Bouëxière for the collection of room-temperature X-ray data and to C. Selfslag for the help with the preparation of the NMR samples. They also thank the Seventh Framework Program of the European Commission and the Joint Advanced Severe Accidents Modelling and Integration for Na-cooled neutron reactors (JASMIN) programme (no. 295803 in FP7). XANES experiments at the ESRF were supported by the European FP7 TALISMAN project, under contract with the European Commission. The authors thank TALISMAN and the ESRF for the provision of beamtime. A.L.S. acknowledges the European Commission and the Ras al Khaimah Centre for Advanced Materials for funding her Ph.D. studentship. G.W. acknowledges Areva for funding his work in the framework of the ParisTech chair of nuclear engineering.

REFERENCES

(1) *GIF R&D Outloook for Generation IV Nuclear Energy Systems*, INIS-FR-11-0958; INIS: Vienna, Austria, 2009; http://www.iaea.org/inis/collection/NCLCollectionStore/_Public/43/002/43002386.pdf.

(2) Housseau, M.; Dean, G.; Perret, F. *Proceedings of the Panel To Discuss the Behaviour and Chemical State of Irradiated Ceramic Fuels*; IAEA: Vienna, Austria, 1974; p 349.

(3) Blackburn, P. E.; Hubbard, W. K. *Proceedings of a Conference on Fast Reactor Fuel Element Technology*; Hindsdale, IL, 1972; p 479.

(4) Housseau, M.; Dean, G.; Marcon, J.-P.; Marin, J. F. *Report CEA-N-1588*; Commissariat à L'énergie Atomique et aux Énergies Alternatives: France, 1973.

(5) Adamson, M. G.; Mignanelli, M. A.; Potter, P. E.; Rand, M. H. *J. Nucl. Mater.* **1981**, *97*, 203−212.

(6) Mignanelli, M. A.; Potter, P. E. *J. Nucl. Mater.* **1983**, *114*, 168−180.

(7) Mignanelli, M. A.; Potter, P. E. *J. Nucl. Mater.* **1984**, *125*, 182−201.

(8) Mignanelli, M. A.; Potter, P. E. *J. Nucl. Mater.* **1985**, *130*, 289−297.

(9) Mignanelli, M. A.; Potter, P. E. *Thermochim. Acta* **1988**, *129*, 143−160.

(10) Strain, R. V.; Bottcher, J. H.; Ukai, S.; Arii, Y. *J. Nucl. Mater.* **1993**, *204*, 252−260.

(11) Scholder, R.; Gläser, H. *Z. Anorg. Allg. Chem.* **1964**, *327*, 15−27.

(12) Bartram, S. F.; Fryxell, R. E. *J. Inorg. Nucl. Chem.* **1970**, *32*, 3701−3706.

DOI: 10.1021/acs.inorgchem.5b00136
Inorg. Chem. 2015, 54, 3552−3561

(13) Marcon, J.-P.; Pesme, O.; Franco, M. *Rev. Int. Hautes Temp Refract.* **1972**, *9*, 193−196.
(14) Lorenzelli, R.; Athanassiadis, T.; Pascard, R. *J. Nucl. Mater.* **1985**, *130*, 298−315.
(15) Pillon, S. *Etude des Diagrammes de Phases U-O-Na, Pu-O-Na et U,Pu-O-Na*. Ph.D. Thesis, Univ. Du Languedoc, 1989.
(16) O'Hare, P. A. G.; Shinn, W. A.; Mrazek, F. C.; Martin, A. E. *J. Chem. Thermodyn.* **1972**, *4*, 401−409.
(17) Osborne, D. W.; Howard, E. F. *J. Chem. Thermodyn.* **1972**, *4*, 411−418.
(18) Fredrickson, D. R.; Chasanov, M. G. *J. Chem. Thermodyn.* **1972**, *4*, 419−423.
(19) Pillon, S.; Ingold, F.; Fischer, P.; Andre, G.; Botta, F.; Stratton, R. W. *J. Nucl. Mater.* **1993**, *206*, 50−56.
(20) Desgranges, L.; Baldinozzi, G.; Rousseau, G.; Nièpce, J.-C.; Calvarin, G. *Inorg. Chem.* **2009**, *48*, 7585−7592.
(21) Rodriguez-Carvajal, J. *Phys. B* **1993**, *192*, 55−69.
(22) Gauthier, C.; Sole, V. A.; Signorato, R.; Goulon, J.; Moguiline, E. *J. Synchrotron Rad.* **1999**, *6*, 164−166.
(23) Ravel, B.; Newville, M. *J. Synchrotron Rad.* **2005**, *12*, 537−541.
(24) Glatzel, P.; Bergmann, U. *Coord. Chem. Rev.* **2005**, *249*, 65−95.
(25) Martel, L.; Somers, J.; Berkmann, C.; Koepp, F.; Rothermel, A.; Pauvert, O.; Selfslag, C.; Farnan, I. *Rev. Sci. Instrum.* **2013**, *84*, 055112.
(26) Wu, G.; Rovnyak, D.; Griffin, R. G. *J. Am. Chem. Soc.* **1996**, *118*, 9326−9332.
(27) Angeli, F.; Charpentier, T.; de Ligny, D.; Cailleteau, C. *J. Am. Ceram. Soc.* **2010**, *93*, 2693−2704.
(28) Benes, O.; Konings, R. J. M.; Wurzer, S.; Sierig, M.; Dockendorf, A. *Thermochim. Acta* **2010**, *509*, 62−66.
(29) Kvashnina, K. O.; Butorin, S. M.; Martin, P.; Glatzel, P. *Phys. Rev. Lett.* **2013**, *111*, 253002.
(30) Keller, C.; Koch, L.; Walter, K. *J. Inorg. Nucl. Chem.* **1965**, *27*, 1205−1223.
(31) Cordfunke, E.; Loopstra, B. *J. Inorg. Nucl. Chem.* **1971**, *33*, 2427−2436.
(32) Morss, L. R. In *Actinides in Perspective: Proceedings of the Actinides—1981 Conference, Pacific Grove, California, USA, 10−15 September, 1981*; Edelstein, N. M., Ed., Pergamon Press: Oxford, 1982; pp 381−407.
(33) Smith, A. L.; Raison, P. E.; Martel, L.; Charpentier, T.; Farnan, I.; Prieur, D.; Hennig, C.; Scheinost, A.; Konings, R. J. M.; Cheetham, A. K. *Inorg. Chem.* **2014**, *53*, 375−382.
(34) Altomare, A.; Cuocci, C.; Giacovazzo, C.; Moliterni, A.; Rizzi, R.; Corriero, N.; Falcicchio, A. *J. Appl. Crystallogr.* **2013**, *46*, 1231−1235.
(35) Schwedes, B.; Hoppe, R. *Z. Anorg. Allg. Chem.* **1972**, *393*, 136−148.
(36) Conradson, S. D.; Manara, D.; Wastin, F.; Clark, D. L.; Lander, G. H.; Morales, L. A.; Rebizant, J.; Rondinella, V. V. *Inorg. Chem.* **2004**, *43*, 6922−6935.
(37) Soldatov, A. V.; Lamoen, D.; Konstantinovic, M. J.; Van den Berghe, S.; Scheinost, A. C.; Verwerft, M. *J. Solid State Chem.* **2007**, *180*, 54−61.
(38) Roof, I. P.; Smith, M. D.; zur Loye, H.-C. *J. Cryst. Growth* **2010**, *312*, 1240−1243.

DOI: 10.1021/acs.inorgchem.5b00136
Inorg. Chem. 2015, 54, 3552−3561